

Flicker Noise as a Probe of Electronic Interaction at Metal–Single Molecule Interfaces

Olgun Adak,[†] Ethan Rosenthal,[‡] Jeffery Meisner,[§] Erick F. Andrade,[§] Abhay N. Pasupathy,[‡] Colin Nuckolls,[§] Mark S. Hybertsen,^{*,||} and Latha Venkataraman^{*,†}

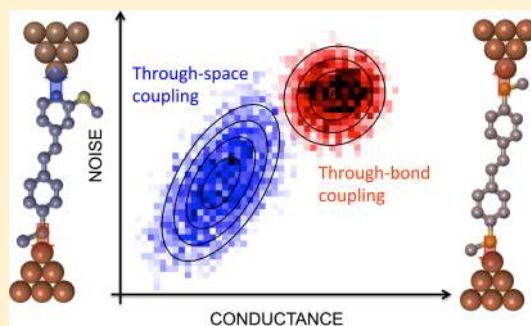
[†]Department of Applied Physics and Applied Mathematics, [‡]Department of Physics, and [§]Department of Chemistry, Columbia University, New York, New York 10027, United States

^{||}Center for Functional Nanomaterials, Brookhaven National Laboratories, Upton, New York 11973, United States

Supporting Information

ABSTRACT: Charge transport properties of metal–molecule interfaces depend strongly on the character of molecule–electrode interactions. Although through-bond coupled systems have attracted the most attention, through-space coupling is important in molecular systems when, for example, through-bond coupling is suppressed due to quantum interference effects. To date, a probe that clearly distinguishes these two types of coupling has not yet been demonstrated. Here, we investigate the origin of flicker noise in single molecule junctions and demonstrate how the character of the molecule–electrode coupling influences the flicker noise behavior of single molecule junctions. Importantly, we find that flicker noise shows a power law dependence on conductance in all junctions studied with an exponent that can distinguish through-space and through-bond coupling. Our results provide a new and powerful tool for probing and understanding coupling at the metal–molecule interface.

KEYWORDS: Single-molecule junctions, flicker noise, $1/f$ noise, through-bond coupling, through-space coupling, density functional theory



For electronic devices based on organic semiconductors, the interaction of molecular orbitals with electronic states of the metal dictates the energy level alignment and electronic coupling, which determine device performance.^{1,2} The physical interactions at such interfaces can lead to electronic coupling that is characterized as either through-bond or through-space. In the former, the hybridization between molecular orbitals and electronic states of the metal occurs through a chemical bond, while in the latter, orbitals responsible for charge transfer do not participate in specific bond formation.³ The most important consequence of this difference is that conductance in systems with through-space coupling is generally lower than in those with through-bond coupling.^{4–6} As a result, performance of devices relying on through-space coupling is often limited by characteristics of the organic–metal interface rather than by the organic constituents.⁷

Here, we investigate the characteristics of flicker noise in a series of nanoscale junctions including gold point contacts and single molecule junctions.^{8–13} We find that flicker noise measurements can clearly differentiate between through-bond and through-space coupling at the single molecule level. We first show that at room temperature, flicker noise in single molecule junctions originates from changes in the molecule–electrode coupling due to electrode atoms switching between metastable configurations. We then demonstrate how scaling of flicker noise with conductance is determined by the relationship

between the electronic transport channel and the mechanical bond to the electrodes. We find that, in tunnel junctions where two electrodes are mechanically decoupled and electronic transport is via through-space tunneling, flicker noise power exhibits a strong dependence on average, individual junction conductance: noise power scales as G^2 . This decreases to a $G^{1.7}$ dependence when we probe a molecular system where both sides are mechanically bonded to the respective electrodes, but through-bond electronic coupling is present on only one side. When single-molecule charge transport is mediated fully by through-bond interactions on both sides, the scaling diminishes to $G^{1.1}$. Finally, for nanoscale gold contacts with $G > 4 \times G_0$, the core of the junction is mechanically and electronically well coupled, and as a result insensitive to nearby fluctuations in structure; conductance fluctuates through changes in the number of channels at the periphery resulting in noise power that scales as $G^{0.5}$. This measurement technique thus enables us to infer the relative contributions of through-space and through-bond coupling at molecule–metal interfaces, providing a new and powerful tool for characterizing these interfaces.

Received: April 1, 2015

Revised: April 30, 2015

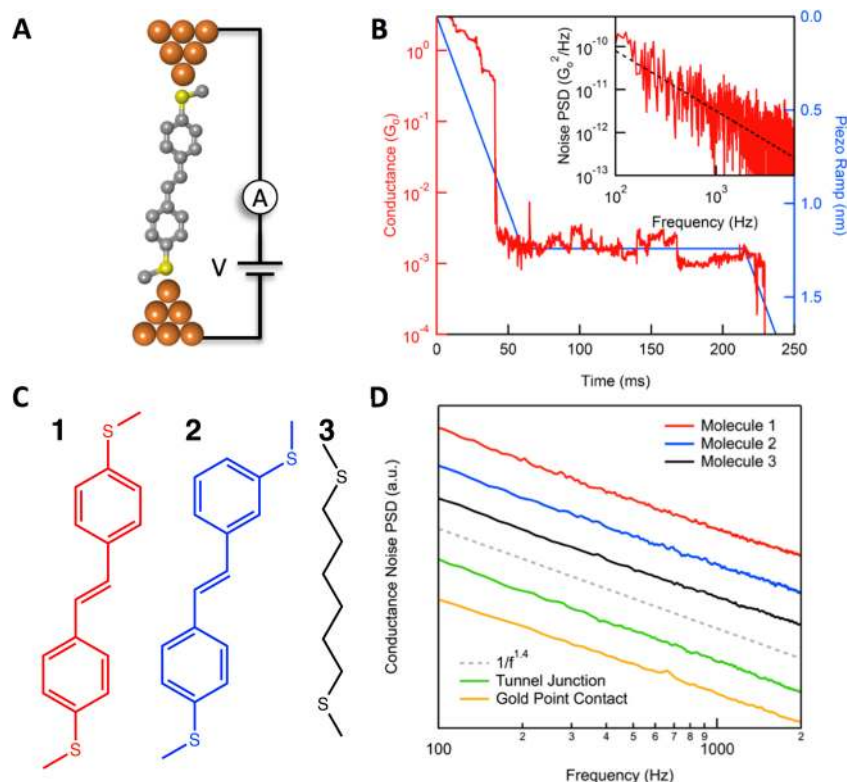


Figure 1. (A) Schematic for molecular junction conductance measurements. (B) Representative conductance and displacement traces for a single noise measurement. Inset: The conductance noise power spectral density obtained by taking square of the discrete Fourier transform of the constant displacement section of conductance trace in B. The dashed line indicates a $f^{-1.4}$ dependence. (C) Chemical structures of the molecules under the study. (D) Averaged conductance noise PSDs for all five systems showing flicker noise along with a line indicating the $f^{-1.4}$ dependence. Traces are offset laterally for clarity.

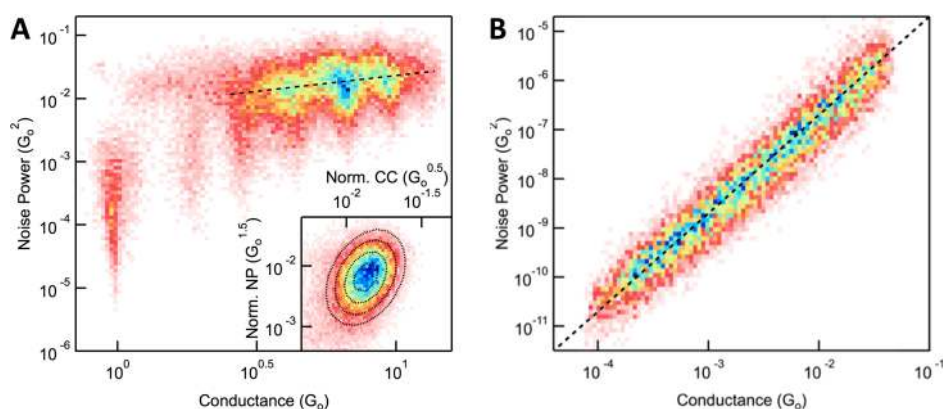


Figure 2. (A) Two-dimensional histogram of flicker noise power against average conductance in gold point contacts. Line overlaid shows a square root dependence. Inset: Two-dimensional histogram of normalized flicker noise power (NP) against normalized conductance change (CC) induced by mechanical oscillation. (B) Two-dimensional histogram of flicker noise power against average conductance in tunnel junctions.

In this work, we use the scanning tunneling microscope based break junction technique (STM-BJ)^{14,15} to characterize conductance noise. In this technique, a gold tip is repeatedly moved in and out of contact with a gold substrate while conductance of the junction is recorded (see Figure 1A for schematic). In order to measure the noise, the junction elongation procedure is paused for 100 ms at a position where prior measurements indicate that a stable junction is likely to form (see Figure 1B). During this time, conductance is recorded at an applied bias of 200 mV using a sampling rate of 100 kHz. Traces that have a conductance within two standard deviations of the molecular conductance histogram peak at the

beginning and the end of this “hold” period are selected for analysis. In order to determine the conductance noise power spectral density (PSD) for a junction, the conductance measured during the fixed displacement section of the junction is analyzed. A discrete Fourier transform of the data is obtained and squared to get the PSD. A sample PSD measured for a 4,4'-di(methylthio)stilbene junction (molecule 1) is shown in the inset of Figure 1B.⁵ This type of noise is often called flicker noise or $1/f$ noise and its presence in single molecule junctions has not yet been explained.^{8–10} In Figure 1D, the conductance PSD, averaged over hundreds of junctions, are shown for tunnel junctions, gold point contacts and three molecules considered

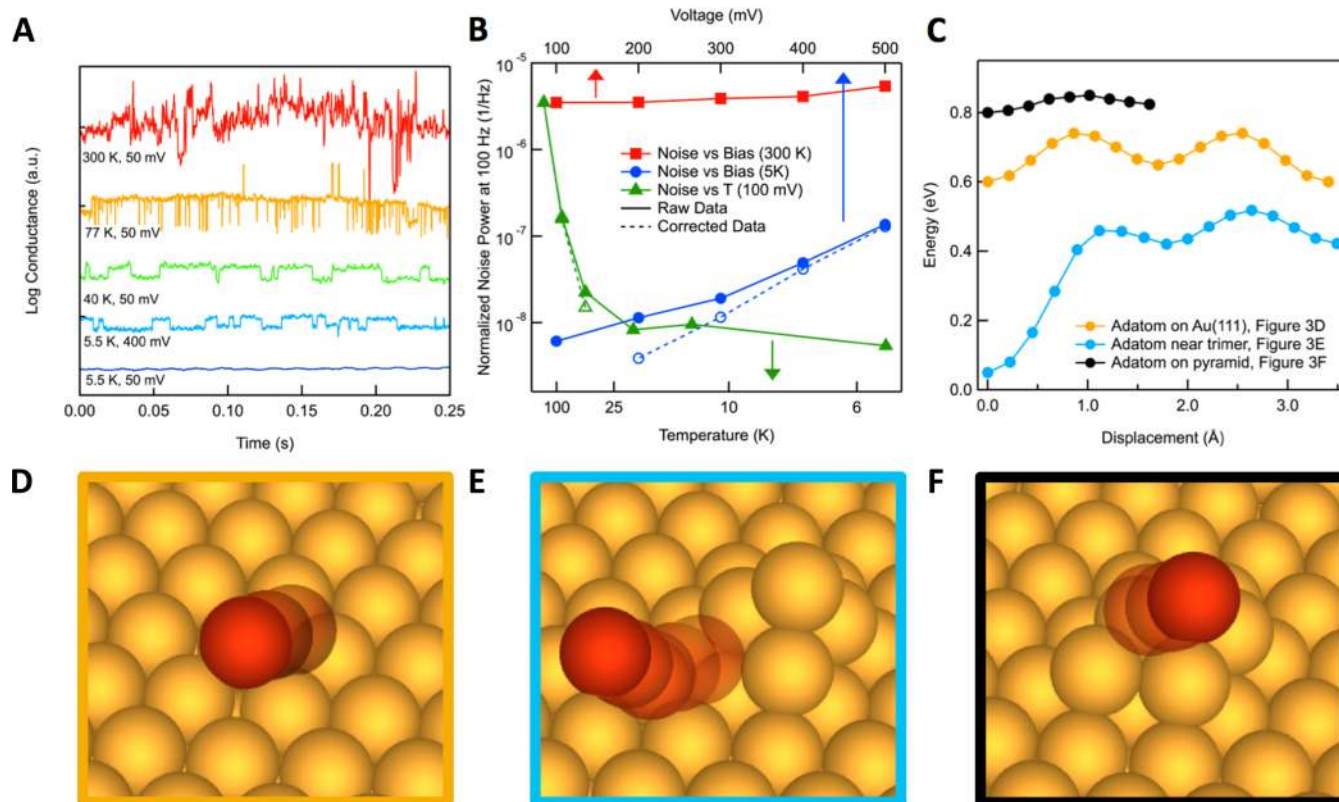


Figure 3. (A) Representative tunnel junction conductance traces (from top to bottom) at 300 K (50 mV), 77 K (50 mV), 40 K (50 mV), 5.5 K (400 mV), and 5.5 K (50 mV). (B) Green: Normalized noise power density plotted against temperature (lower axis) at 100 mV bias. Normalized noise power density at 100 Hz versus bias voltage (top axis) at 300 K (red) and at 5.5 K for junctions with a conductance of $10^{-3} G_0$ (blue). Filled shapes represent the measured values, empty shapes with dashed connecting lines represent the values after background subtraction. Note that for the data taken at 300 K, background subtraction does not change the values significantly. (C) Potential energy profiles calculated using a density function theory approach for a series of three illustrative structures and gold atom movements: (D) Adatom diffusion pathway on the close packed (111) surface from fcc to hcp to neighboring fcc hollow sites (yellow data in C); (E) Dissociation of a five atom asperity into a four atom pyramid and an adatom, first to an hcp site and then to a neighboring fcc site (blue data in C); (F) Switching of an apical adatom in a five atom asperity between a local fcc and hcp sites (black data in C). Curves are offset for clarity; only relative energies within each curve are meaningful.

here (see Figure 1C for structures). At room temperature, the noise power shows a $f^{-1.4}$ frequency dependence. The frequency dependence of flicker noise power is identical in all five systems indicating that the source of the flicker noise is related to the electrodes and not the system bridging the electrodes. (As detailed in the Supporting Information, Figures S1 and S2, the observed flicker noise is not due to electronic or mechanical effects in our setup.)

We hypothesize that flicker noise in all three systems arises from configuration changes in electrode structure due to electrode atoms proximal to the junction fluctuating between metastable positions. As the measured noise shows a clear $f^{-1.4}$ dependence, we can rule out any suppression in noise due to quantum interference effects and shot noise.¹² Such fluctuations have been shown to cause two-level conductance fluctuations in both tunnel junctions and metallic point contacts at temperatures ranging from 7 to 100 K.^{16–18} We therefore argue that room temperature flicker noise is a consequence of many accessible two level conductance fluctuations, with average switching rates distributed over the measurement bandwidth, which would result in noise power spectrum with a $1/f^n$ frequency dependence.¹⁹

To verify this hypothesis, we first examine the flicker noise in gold point contacts with conductance ranging from 1 to 10 G_0 at room temperature. To quantify noise, we numerically

integrate the PSD from 100 Hz to 1 kHz for every junction and take this value as the measure of flicker noise a junction experiences. The 1 kHz upper limit in the frequency range is chosen because the thermal noise of the current amplifier becomes comparable to flicker noise at frequencies above this cutoff. The lower limit is chosen considering mechanical drifts in the experimental setup; such drifts result in a $1/f^2$ frequency dependence, which become comparable to flicker noise at low frequencies. In Figure 2A, we make a two-dimensional histogram of the integrated flicker noise against the average conductance for 50 000 gold-point contacts. We find that the integrated flicker noise power dips near integer multiple of G_0 which is not surprising because junctions with fully open conductance channels have a transmission that is less sensitive to junction structure.²⁰ The dips occur at conductance values that are slightly lower than integer multiples of G_0 due to an effective series resistance caused by scattering centers near the contact.²¹ We also note that the noise power scales as $G^{0.5}$ for contacts with a conductance greater than $\sim 4 G_0$. To probe this further, we compare the relation between flicker noise and the change in conductance when we perturb the junction with an external oscillatory mechanical perturbation (see Figure S3). We find that junctions that are less susceptible to conductance changes upon mechanical perturbation experience less flicker noise (see Figure 2A inset).

This is consistent with our hypothesis that flicker noise arises due to configuration changes in the electrode structure. In contrast to gold point-contacts, flicker noise in tunnel junctions that form after the rupture of the gold point-contact show a different relation to average conductance. We measure flicker noise for 10,000 tunnel junctions with G_{AVG} ranging from $10^{-4} G_0$ to $10^{-1.4} G_0$ and show a two-dimensional histogram of the noise power against G_{AVG} in Figure 2B. We observe a clear quadratic dependence with noise power scaling as G^2 .

To understand the observed scaling of the noise power, we consider the impact of fluctuations in metal atom positions in these junctions. For the case of the tunnel junctions, the junction gap size effectively fluctuates due to the position of atoms on either electrode near the area of closest approach between tip and substrate. Since these tunneling gaps are probed right after a rupture event, the current is exponentially sensitive to the overall gap width in general, but also to the position of just a few metal atoms that effectively define it, as would be expected from the atomic resolution in a scanning tunneling microscope in the regime of an atomically sharp tip. The conductance of a tunnel junction can be written as $G = G_c e^{-bz} = G_c e^{-bz_0} e^{-b(z-z_0)}$ where b is the decay constant, z is the effective gap size that fluctuates around a mean value z_0 , and G_c is a constant. The scale of fluctuations in z is bounded and independent of the average gap z_0 , and therefore also of $G_{AVG} = G_c e^{-bz_0} \langle e^{-b(z-z_0)} \rangle$ with $e^{-b(z-z_0)} / \langle e^{-b(z-z_0)} \rangle$ describing the fluctuations around G_{AVG} . It then follows that the noise amplitude (noise in $G = G_{AVG} (e^{-b(z-z_0)} / \langle e^{-b(z-z_0)} \rangle)$) scales with G_{AVG} and the noise power scales as G_{AVG}^2 . This result can be easily derived under the assumption of Gaussian fluctuations in z (see the Supporting Information), although it applies to fluctuations that follow more general distributions. On the other hand, for the gold point-contact, the conductance scales approximately with the number of atoms in the junction cross-section area. If fluctuations are limited to a single atom, then the noise power is independent of G_{AVG} . However, the entire perimeter is open for fluctuations. Assuming each fluctuating center is independent, the number of possible centers will scale with the square root of the number of atoms in the contact and the noise power scales as $G^{0.5}$ as observed for contacts with a conductance greater than $4G_0$ (see the Supporting Information).

To check further the validity of our model, we measure the temperature dependence of the flicker noise in tunnel junctions and gold point-contacts under ultrahigh vacuum conditions. Since the switching of atoms between metastable positions is a thermally activated process, at sufficiently low temperatures, single two-level conductance fluctuations should be discernible. We show, in Figure 3A, sample conductance versus time traces measured for stable tunnel junctions at temperatures ranging from 5.5 to 300 K. Flicker noise is clearly visible at room temperature but decreases substantially upon cooling. At 40 K, single two-level conductance fluctuations are visible; at 5.5 K, no noise is seen. To quantify this result in a statistically significant way, we collect conductance-time traces for over 10000 different tunnel junctions at each temperature. We obtain the noise power density at 100 Hz, instead of numerically integrating up to 1 kHz because the electronic and mechanical noise features appear in the spectrum at low temperatures due to suppressed flicker noise. We normalize this by G_{AVG}^2 to remove the conductance dependence and plot the result averaged over 10000 traces against temperature in Figure 3B. We see that the flicker noise power decreases rapidly with decreasing temperature attaining the experimental noise floor

below 40 K. We take the average of the values obtained below 40 K as representative of the experimental noise floor and subtract this from measurements at higher temperatures and higher voltages. An exponential decrease in noise down to 40 K with increasing inverse temperature ($1/T$) is visible in Figure 3B. Such a decrease is typical for a thermally activated two-level systems.²² Furthermore, we observed a strong bias voltage dependence of flicker noise in tunnel junctions at 5.5 K but not at 300 K (see Figure 3A and 3B).²³ As detailed in the Supporting Information, the observed voltage dependence can be fit with a model where bias voltage electrostatically lowers the potential barrier for the two-level fluctuations (see also Supporting Information, Figure S4A).²⁴ Taken together, these experimental results show clearly that fluctuations in the position of atoms on the electrodes cause the observed flicker noise. More importantly, the activation energies for these fluctuations have a broad energy distribution as they are observed within the experimental bandwidth over a wide temperature range.

To get more insight into the kinetic processes that can result in such fluctuations in the junction, we use density functional theory (DFT) based calculations, as implemented in the VASP package,^{25–28} to simulate the potential surface for atomic-scale fluctuations in gold asperities (as detailed in the Supporting Information). We first consider the diffusion of an adatom on a close-packed (111) surface. The fcc hollow site is most stable for the adatom. Diffusion from one fcc hollow site to another goes through a metastable hcp hollow site. As shown in Figure 3C, we find a primary barrier of 0.14 eV (fcc to hcp) and a secondary barrier of 0.09 eV (hcp to fcc) for this diffusion path that is illustrated in Figure 3D. This shows that in the simplest geometry considered, there are two accessible states that have different lifetimes. Since we expect the experimental tip and substrate structures to be more complex with additional roughness, we also explored the affinity of the adatom to other local clusters. For example, Figure 3E shows that an adatom is bound to a site adjacent to a four-atom pyramid. Once bound, fluctuations away from this state are controlled by a relatively large barrier (0.4 eV) while the barrier for return is rather small (0.04 eV). Furthermore, the calculations show that the specific size of these barriers depends on the cluster geometry and the neighboring structures. This example suggests a physical mechanism for the fluctuations in Figure 3A that appear as spikes (yellow trace measured at 77 K), having asymmetric lifetimes for the two states involved. Finally, with the idea that rather sharp asperities can survive longer at the lower temperatures probed here, we show an example of an adatom fluctuating at the tip of such an asperity (Figure 3F), where the forward barrier is about 0.05 eV and the reverse barrier is less than 0.03 eV. The reduced energy scale follows from the lower overall coordination of the atoms involved.

Unlike tunnel junctions, gold point contacts do not exhibit any two-level conductance fluctuations at 77 K under 100 mV bias voltage implying that atomic fluctuations that alter junction structure have substantially increased activation energies. Increasing the bias voltage, however, does result in two-level conductance fluctuations in gold point contacts at 77 K (see Supporting Information, Figure S4). We do not attempt to distinguish between local heating and electrostatic effects of bias voltage induced increase in flicker noise for these point-contacts. However, we note that the room temperature flicker noise at 50 mV in atomic contacts is greater than the noise at 77 K at a 400 mV bias voltage (see Supporting Information),

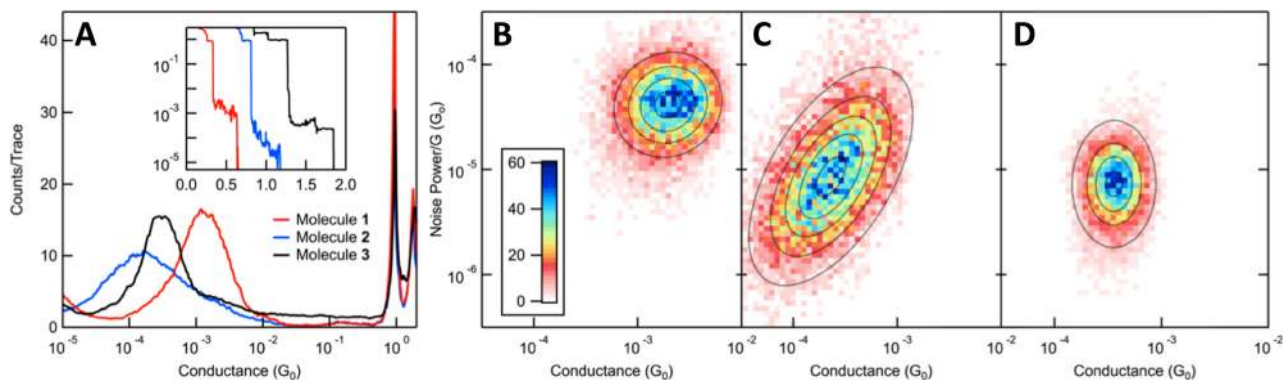


Figure 4. (A) Conductance histograms of molecule 1, molecule 2, and molecule 3. Inset: sample traces. (B–D) Two-dimensional histogram of normalized flicker noise power against average junction conductance for molecule 1 (B), molecule 2 (C), molecule 3 (D). Dotted contours represent fits to the bivariate normal distribution.

while the local electronic temperature in $3 G_0$ to $5 G_0$ gold point contacts has been shown to increase by 300 K under 300 mV bias voltage at room temperature.²⁹ This means that bias induced local hot electron population can be achieved at the apex without elevating the lattice temperature significantly, possibly because the electron–electron scattering length is smaller than electron–phonon scattering length in gold.³⁰

We now turn to single molecule junctions and examine flicker noise characteristics of three molecular systems, 4,4'-di(methylthio)stilbene (molecule 1), 3,4'-di(methylthio)stilbene (molecule 2) and 2,9-dithiadecane (molecule 3) at room temperature. Molecules 1 and 2 are synthesized as described previously⁵ and 3 is obtained from Alfa-Aesar and used without further purification. Molecule 1 forms stable Au–single-molecule–Au junctions through Au–S donor–acceptor bonds with a conductance around $1.3 \times 10^{-3} G_0$ as shown in Figure 4A in agreement with previous measurements.⁵ Molecule 2 also forms single-molecule junctions that are mechanically anchored through two Au–S donor–acceptor bonds. However, at the meta-linker, through-bond conduction is suppressed due to destructive interference effects since the orbital that dominates transport in these systems, the highest occupied molecular orbital (HOMO), does not have any weight on the meta-linker.^{31,32} As a result, charge transfer is mediated by through-space interaction on the meta-side, and through-bond at the other which reduces the conductance to $1.6 \times 10^{-4} G_0$.⁵ Molecule 3 is an alkane terminated with methylsulfide linkers that conducts by through-bond tunneling via its σ -system. Its conductance is peaked around $3.1 \times 10^{-4} G_0$, significantly smaller than that of 1 where the π -system mediates the charge transport.

To examine the noise in these systems, we measure the conductance of more than 10,000 stable junctions for each molecular system at a 200 mV bias voltage. For the noise analysis, we follow the same procedure illustrated in Figure 1, parts B and C at room temperature and calculate the noise power between 100 Hz and 1 kHz for each junction by numerically integrating the PSD. In Figure 4B–D, we show a two-dimensional histogram of integrated flicker noise power normalized by G_{AVG} against G_{AVG} for 1, 2, and 3. We see that the normalized flicker noise power in 1 and 3 is insensitive to junction conductance, while that of 2 correlates strongly with junction conductance. Quantitatively, the noise power in 1 and 3 scales with $G^{1.1}$ and $G^{1.0}$ respectively. In 2, the noise power scales with $G^{1.7}$, which is interestingly close to the results of the tunnel junctions (see Supporting Information and Figure S5 for

analysis details). As shown in the Supporting Information, Figure S6, for two additional molecules, we find that through-bond coupled molecular junctions show a noise power scaling close to $G^{1.2}$, while for junctions with one through-bond and one through-space coupling, it scales with $G^{1.7}$.

In order to understand this result, we consider the simplest model for transport in a single-molecule junction³³ where conductance is determined by the energy level alignment of the conducting orbital with the electrode Fermi energy (ΔE) and its electronic coupling to the electrodes (Γ). While both play a role, the coupling Γ is strongly influenced by electrode structure, binding geometry and conformational changes in molecular structure.^{34–38} In particular, Γ changes appreciably for different tip structures on the electrodes,³⁵ so fluctuations in the Au atoms between metastable positions in the electrode will result in a change in the junction conductance. For a through-bond coupled molecule, we can assume that fluctuations in Γ are independent of Γ as there is a mechanical constraint that maintains the electrode–molecule separation. For a through-space coupled molecule, fluctuations in Γ are proportional to Γ because Γ decreases exponentially with the distance between the molecule and the electrode site (see Supporting Information). With these assumptions, it can be analytically shown that the flicker noise power in a molecular junction with through-bond coupling at both ends scales with average conductance of the molecular junction explaining the behavior of 1 and 3. In contrast, for a molecular junction with through-space coupling at both ends, flicker noise power scales with the square of average conductance (see Supporting Information for analytic derivation). This is what we obtain experimentally for the tunnel junctions, a through-space coupled system.

Molecule 2 is a hybrid system with both through-bond and through-space coupling. For such a system, it is not possible to obtain an analytical expression for the relation between noise and conductance. Through a Monte Carlo simulation, we find that the noise scaling in this hybrid system is determined by the linker that controls the junction-to-junction variations in conductance (see Supporting Information, Figure S7). Specifically, if through-space coupling has a larger variation, the noise scaling is closer to that of a tunnel junction, while if the through-bond coupling has a larger variation, the noise scaling is closer to that of a through-bond coupled junction. Interestingly, if through-space and through-bond couplings have the same distribution, the scaling exponent turns out to be 1.5 regardless of the mean through-space and through-bond coupling. This is intuitive as through-space coupled molecular

junctions exhibit a broader distribution of conductance compared with the through-bond coupled junction as can be seen in Figure 4A. The example of **2**, with a scaling exponent 1.7, must have a distribution of through-space coupling that is wider than that of through-bond coupling.

In general, we note that there can be other aspects of the junction structure that fluctuate and contribute to noise, possibly leading to changes in both Γ and ΔE , including rotational degrees of freedom of the molecule or the linker attachment itself and changes to the local electrostatic potential that affect ΔE . For molecules **1** and **2**, the twisting of molecular backbone is hindered by the presence of C=C double bond in stilbene backbone so that internal rotations do not contribute to noise.³⁹ Although rotations about the Au–S–C torsion angle are possible, the activation energy is very small⁴⁰ and thus the conductance changes due to these rotations would only be seen at frequencies higher than our instrument bandwidth. Indeed, measurements of a control molecule that does not accommodate changes to the Au–S–C torsion angle (see Supporting Information Figure S8) show that noise power scales as $G^{1.2}$, consistent with the results of molecule **1**. Breaking and reattachment of the Au–S donor–acceptor bond, with an energy around 0.6 eV could contribute to the measured noise.^{22,40} However, as detailed in Supporting Information, we do not find any evidence of reattachment within the 100 ms time-scale of the measurement. Finally, we note that linkers can switch between metastable binding sites on the electrode.³⁷ Since this can be modeled as a change in Γ for the junction, it does not yield a separate source of noise for the molecular junctions.

In conclusion, we show that the flicker noise observed at room temperature in molecular junctions, gold point-contacts and tunnel junction is due to many two-level positional switching of electrode atoms. We demonstrate how the character of the electronic coupling in single-molecule junctions determines the flicker noise–conductance relation. Specifically, we show that through-bond coupling leads to linear noise–conductance relation, while through-space coupling results in quadratic one. This gives us ability to distinguish between through-space and through-bond coupling at metal–organic interfaces without referring to electronic structures.

■ ASSOCIATED CONTENT

● Supporting Information

Experimental and theoretical details and additional data. The Supporting Information is available free of charge on the ACS Publications website at DOI: 10.1021/acs.nanolett.5b01270.

■ AUTHOR INFORMATION

Corresponding Authors

*(L.V.) E-mail: lv2117@columbia.edu.

*(M.S.H.) E-mail: mhyberts@bnl.gov.

Notes

The authors declare no competing financial interest.

■ ACKNOWLEDGMENTS

The experimental portion of this work was supported by the NSF under Award DMR-1122594. A portion of this work was performed using facilities in the Center for Functional Nanomaterials, which is a U.S. DOE Office of Science User Facility, at Brookhaven National Laboratory under Contract

No. DE-SC0012704. E.R. and A.N.P. were supported by NSF-DMR 1056527.

■ REFERENCES

- (1) Braun, S.; Salaneck, W. R.; Fahlman, M. *Adv. Mater.* **2009**, *21*, 1450–1472.
- (2) Cahen, D.; Kahn, A. *Adv. Mater.* **2003**, *15*, 271–277.
- (3) Hoffmann, R. *Acc. Chem. Res.* **1971**, *4*, 1–9.
- (4) Wu, S. M.; Gonzalez, M. T.; Huber, R.; Grunder, S.; Mayor, M.; Schonenberger, C.; Calame, M. *Nat. Nano.* **2008**, *3*, 569–574.
- (5) Meisner, J. S.; Ahn, S.; Aradhya, S. V.; Krikorian, M.; Parameswaran, R.; Steigerwald, M.; Venkataraman, L.; Nuckolls, C. *J. Am. Chem. Soc.* **2012**, *134*, 20440–20445.
- (6) Engelkes, V. B.; Beebe, J. M.; Frisbie, C. D. *J. Am. Chem. Soc.* **2004**, *126*, 14287–14296.
- (7) Tulevski, G. S.; Miao, Q.; Afzali, A.; Graham, T. O.; Kagan, C. R.; Nuckolls, C. *J. Am. Chem. Soc.* **2006**, *128*, 1788–1789.
- (8) Ochs, R.; Secker, D.; Elbing, M.; Mayor, M.; Weber, H. B. *Faraday Discuss.* **2006**, *131*, 281–289.
- (9) Tsutsui, M.; Taniguchi, M.; Kawai, T. *Nat. Commun.* **2010**, *1*, 138.
- (10) Sydoruk, V. A.; et al. *J. Appl. Phys.* **2012**, *112*, 014908.
- (11) Xiang, D.; Lee, T.; Kim, Y.; Mei, T.; Wang, Q. *Nanoscale* **2014**, *6*, 13396–13401.
- (12) Ludoph, B.; Ruitenbeek, J. M. v. *Phys. Rev. B* **2000**, *61*, 2273–2285.
- (13) van den Brom, H. E.; van Ruitenbeek, J. M. *Phys. Rev. Lett.* **1999**, *82*, 1526–1529.
- (14) Xu, B. Q.; Tao, N. J. *Science* **2003**, *301*, 1221–1223.
- (15) Venkataraman, L.; Klare, J. E.; Nuckolls, C.; Hybertsen, M. S.; Steigerwald, M. L. *Nature* **2006**, *442*, 904–907.
- (16) Sperl, A.; Kröger, J.; Berndt, R. *Phys. Rev. B* **2010**, *81*, 035406.
- (17) Tsutsui, M.; Kurokawa, S.; Sakai, A. *Appl. Phys. Lett.* **2007**, *90*, 133121.
- (18) Hubert, K.; Thomas, L.; Remi, Z.; Philippe, D.; Andrés, S. *Nanotechnology* **2012**, *23*, 235707.
- (19) Hooge, F. N.; Bobbert, P. A. *Physica B* **1997**, *239*, 223–230.
- (20) Armstrong, J.; Schaub, R.; Hua, S.; Chopra, H. *Phys. Rev. B* **2010**, *82*, 195416.
- (21) Agrait, N.; Yeyati, A. L.; van Ruitenbeek, J. M. *Phys. Rep.* **2003**, *377*, 81–279.
- (22) Hänggi, P.; Talkner, P.; Borkovec, M. *Rev. Mod. Phys.* **1990**, *62*, 251–341.
- (23) Todorov, T. N. *Philos. Mag. B* **1998**, *77*, 965–973.
- (24) Muller, C. J.; van Ruitenbeek, J. M.; de Jongh, L. J. *Phys. Rev. Lett.* **1992**, *69*, 140–143.
- (25) Perdew, J. P.; Burke, K.; Ernzerhof, M. *Phys. Rev. Lett.* **1996**, *77*, 3865–3868.
- (26) Kresse, G.; Furthmüller, J. *Phys. Rev. B* **1996**, *54*, 11169.
- (27) Kresse, G.; Joubert, D. *Phys. Rev. B* **1999**, *59*, 1758–1775.
- (28) Blochl, P. E. *Phys. Rev. B* **1994**, *50*, 17953–17979.
- (29) Chen, R.; Wheeler, P. J.; Natelson, D. *Phys. Rev. B* **2012**, *85*, 235455.
- (30) Kanter, H. *Phys. Rev. B* **1970**, *1*, 522–536.
- (31) Aradhya, S. V.; Meisner, J. S.; Krikorian, M.; Ahn, S.; Parameswaran, R.; Steigerwald, M. L.; Nuckolls, C.; Venkataraman, L. *Nano Lett.* **2012**, *12*, 1643–1647.
- (32) Batra, A.; Meisner, J. S.; Darancet, P.; Chen, Q.; Steigerwald, M. L.; Nuckolls, C.; Venkataraman, L. *Faraday Discuss.* **2014**, *174*, 79–89.
- (33) Paulsson, M.; Datta, S. *Phys. Rev. B* **2003**, *67*, 241403.
- (34) Basch, H.; Cohen, R.; Ratner, M. A. *Nano Lett.* **2005**, *5*, 1668–1675.
- (35) Quek, S. Y.; Venkataraman, L.; Choi, H. J.; Louie, S. G.; Hybertsen, M. S.; Neaton, J. B. *Nano Lett.* **2007**, *7*, 3477–3482.
- (36) Tian, W.; Datta, S.; Hong, S.; Reifenberger, R.; Henderson, J. I.; Kubiak, C. P. *J. Chem. Phys.* **1998**, *109*, 2874–2882.
- (37) Kamenetska, M.; Koentopp, M.; Whalley, A.; Park, Y. S.; Steigerwald, M.; Nuckolls, C.; Hybertsen, M.; Venkataraman, L. *Phys. Rev. Lett.* **2009**, *102*, 126803.

- (38) Donhauser, Z. J.; et al. *Science* **2001**, *292*, 2303–2307.
- (39) Mulliken, R. S.; Roothaan, C. C. J. *Chem. Rev.* **1947**, *41*, 219–231.
- (40) Park, Y. S.; Widawsky, J. R.; Kamenetska, M.; Steigerwald, M. L.; Hybertsen, M. S.; Nuckolls, C.; Venkataraman, L. *J. Am. Chem. Soc.* **2009**, *131*, 10820–10821.